Theor Chem Acc (2011) 128:377–388
DOI 10.1007/s00214-010-0881-9

REGULAR ARTICLE

Interaction of chemically modified tetracyclines with catalytic Zn(II) ion in matrix metalloproteinase: evidence for metal coordination sites

Bruna L. Marcial · Luiz Antônio S. Costa · Wagner B. De Almeida · Cleber P. A. Anconi · Hélio F. Dos Santos

Received: 21 September 2010 / Accepted: 22 December 2010 / Published online: 6 January 2011

Abstract Chemically modified tetracyclines (CMTs) have shown promising activity as matrix metalloproteinase (MMP) inhibitors acting as zinc-binding groups. The first step in the design of new and effective drugs is the molecular description of the mechanism of action in chemical and biological environments. In the present study, the structure and stability of $[Zn(LH_n)(H_2O)_2]^{2-x}$ ($n = 0$, 1, 2 and $x = -2$, -1, 0) and $[Zn(L)(His)_3]$, where L represents five distinct, structurally related CMTs, are discussed. In addition to the effect of the ligand on Zn(II) coordination, the role of the solvent and pH was also determined. The results suggested that O1–Oam (labeled as site II in the present paper) of CMT-1, CMT-4 and CMT-7 was the most stable site in the gas phase and aqueous solution. However, for CMT-3 and CMT-8, coordination at the O11–O12 moiety (site VI) was preferred. This coordination site is an essential binding mode of CMTs with active zinc in the MMP catalytic site; therefore, our results support the singular behavior of CMT-3 and CMT-8 as promising MMP inhibitors.

Keywords Tetracycline · DFT calculations · Matrix metalloproteinase · Chemically modified tetracycline

Electronic supplementary material The online version of this article (doi:10.1007/s00214-010-0881-9) contains supplementary material, which is available to authorized users.

B. L. Marcial · L. A. S. Costa · H. F. Dos Santos (✉)
Núcleo de Estudos em Química Computacional (NEQC), Departamento de Química, ICE, Universidade Federal de Juiz de Fora, Juiz de Fora, MG 36036-330, Brazil
e-mail: helio.santos@ufjf.edu.br

W. B. De Almeida
Laboratório de Química Computacional e Modelagem Molecular (LQC-MM), Departamento de Química, ICEx, Universidade Federal de Minas Gerais, Belo Horizonte, MG 31270-901, Brazil

C. P. A. Anconi
Departamento de Química, Universidade Federal de Lavras, Campus Universitário, 3037, Lavras, MG 37200-000, Brazil

H. F. Dos Santos
Núcleo de Bioinformática de Juiz de Fora (NuBio-JF), Universidade Federal de Juiz de Fora, Juiz de Fora, MG 36036-330, Brazil

1 Introduction

Matrix metalloproteinases (MMPs) are a family of Ca(II)- and Zn(II)-dependent proteinases that proteolytically degrade extracellular matrix components [1] and are involved in essential physiological and pathological processes in the human body. Many studies have shown that MMPs play a significant role in tumor invasion, metastasis and angiogenesis [2]. Thus, inhibition of MMP activity is an interesting therapeutic strategy for the treatment of diseases such as cancer. In recent years, a number of MMP inhibitors (MMPIs) have been developed [3]; however, clinical trial results have been predominantly unfavorable [4, 5]. As a result, a significant effort has been extended toward identifying specific inhibitors with distinct zinc-binding groups (ZBGs) [6]. The most studied synthetic MMP inhibitors containing ZBGs belong to the hydroxamate family, which covalently bind to the zinc atom at the MMP active site [7]. An alternative class of potential MMP inhibitors is tetracycline (TC) derivatives, which have been evaluated in preclinical cancer models and have shown promising results [8, 9].

TC derivatives that show MMP inhibition activity include tetracycline-based antibiotics such as tetracycline (TC), minocycline and doxycycline (DOX, the only

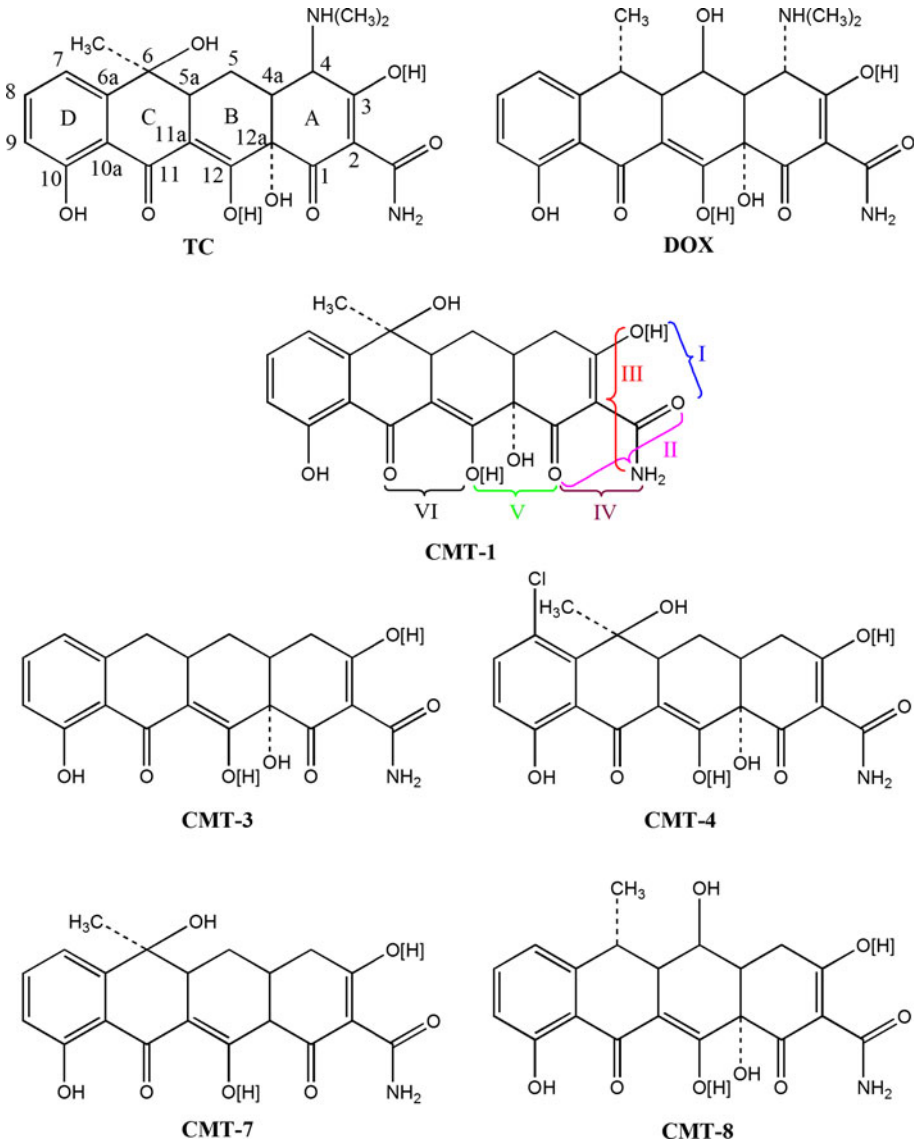

Fig. 1 Structures of tetracycline (*TC*), doxycycline (*DOX*) and their chemically modified analogs (CMT-*n*). The numbering scheme and the coordination sites are shown; I (O3–Oam), II (O1–Oam), III (O3–Nam), IV (O1–Nam), V (O12–O1) and VI (O11–O12). The site VI is available only at high pH, where the fully deprotonated form is favored

FDA-approved MMPI [1, 5]), and chemically modified tetracycline (CMTs) [10, 11] (Fig. 1). CMTs are a new family of at least ten molecules (CMT-1 to 10) that lack a dimethylamino (DMA) group at the C4 position of the A ring in TC. Due to the absence of this functional group, CMTs do not present antimicrobial activity [12]. However, some CMTs are more potent MMP inhibitors than conventional antimicrobial TCs [13]. CMTs have several advantages over the parent TCs, such as lower systemic toxicity and higher plasma accumulation, allow for reduced doses. In addition, CMTs do not result in resistant microorganisms, which is a common effect of antibiotic therapy [9, 14, 15]. The mechanism of MMP inhibition by tetracyclines is not completely understood at the molecular level. However, tetracyclines are known to bind to Zn(II) or Ca(II) ions associated with MMP and can block the active site and induce conformational changes that render the pro-enzyme susceptible to fragmentation during the activation process. According to Acharya et al. [8], CMTs reduce active MMP or pro-MMP through the aforementioned mechanism. 6-demethyl-6-deoxy-4-dedimethylamino tetracycline, also known as CMT-3 (Col-3) (Fig. 1), is one of the most active CMTs [6, 16]. Several studies in the literature have discussed the efficacy of CMT-3, and evidence suggests that CMT-3 has antitumor and anti-metastasis activity [9, 14]. CMT-3 inhibits the expression and activity of MMP-2 and MMP-9, and gelatinases A and B, respectively [2], which are responsible for degrading basement membrane type IV collagen and are essential for cellular invasion. Thus, these enzymes play a primary role in tumor progression. Other CMTs also have an effect on gelatinase A and B activity, including CMT-1, CMT-4, CMT-7 and CMT-8 (Fig. 1), where the latter is a direct derivative of DOX tetracycline. The distinct efficacy of CMTs as MMP

inhibitors may result from their structural differences, which can alter the solubility and reactivity of these compounds.

The application of theoretical methods to investigate structural aspects and thermodynamic properties of metal complexation processes is relevant for the elucidation of the action mode of CMTs as MMPIs. Moreover, theoretical studies can provide valuable results on the reactivity of different CMTs [17]. TC derivatives such as CMTs possess several metal binding sites and are able to complex metal ions such as Mg(II), Ca(II), Zn(II), Al(III) and Pt(II) [18–24], which may directly interfere with the mechanism of action of these compounds at the molecular level. Our group and many others [25–29] have contributed to the understanding of tetracycline chemistry by applying theoretical methods to investigate conformational and tautomeric equilibria, metal ion complexation and spectroscopic properties [30–35]. These studies have assisted experimentalists in elucidating the coordination modes of metal ions such as Al(III), Mg(II) and Pt(II), which is a difficult task due to the existence of several possible coordination sites.

The present study aims to apply first principles quantum chemistry calculations based on density functional theory (DFT) to describe interactions between different CMTs (Fig. 1) and the Zn(II) ion in MMP enzymes. First, we considered the interaction of CMTs with Zn(II)-hexahydrated species ($[Zn(H_2O)_6]^{2+}$) at distinct coordination modes, including sites I–VI shown in Fig. 1. Next, we included the first coordination shell from the active site of MMP-9 in the molecular model, and accounted for His401, His405, and His411, which were identified from a high-resolution X-ray crystallographic structure (PDB code 1L6J) [36]. Finally, the structure and stability of CMT–Zn(II) complexes are discussed. The present report is the first theoretical attempt to investigate the mechanism of action of tetracycline MMP inhibitors.

2 Theoretical treatments

The CMTs considered in the present study included CMT-1, CMT-3, CMT-4, CMT-7 and CMT-8 (see Fig. 1). Compared to other CMTs and the parent tetracyclines, the CMTs evaluated in the current investigation are relatively lipophilic [15] and are better absorbed by the organism and human cells after oral administration. Unlike native TC, which possesses a third pKa, the CMTs contain only two ionizable groups [37]. As a result, the molecules can exist in the non-ionized (LH_2) and ionized form (LH^- at O3, pKa1 = 5.6 ± 0.2 and L^{2-} at O3 and O12, pKa2 = 8.35 ± 0.07), depending on the pH of the solution.

The present study was organized into two parts. First, the coordination modes represented in Fig. 1 were tested for CMT-1 and CMT-3. The former presents the closest geometry to the parent TC, and the latter is the simplest CMT. In addition to the distinct coordination modes, we considered the geometries of the free ligands in their ionized forms (LH_2, LH^- and L^{2-}) and the hydrated Zn(II) coordination shell, as shown in Eq. 1.

$$\left[Zn(H_2O)_6\right]^{2+} + LH_n^x \rightarrow \left[Zn(LH_n)(H_2O)_2\right]^{2-x} + 4H_2O$$
$$\therefore n = 0, 1, 2 \quad \text{and} \quad x = -2, -1, 0 \tag{1}$$

In the second part of the study, the most stable coordination modes of CMT-1–Zn(II) and CMT-3–Zn(II) complexes were considered, and a model of the amino acids in the active site of MMP-9 was constructed. The X-ray crystallographic structure [36] was applied, and only the first coordination sphere of active zinc in the metalloproteinase (His401, His405 and His411) was considered. Neutral amino acid structures with COOH and NH_2 groups were employed, and all of the CMTs (CMT-1, CMT-3, CMT-4, CMT-7 and CMT-8) were used as ligands in the L^{2-} ionized form. Thus, the final stoichiometry of the complexes was $[Zn(L)(His)_3]$.

Using DFT and hybrid B3LYP functional [38, 39], the geometries were fully optimized and characterized as true minima on the gas phase potential energy surface (PES). The standard split valence basis set 6-31G(d) was used for all of the atoms, including zinc [40, 41]. Recently, Ramos et al. [42, 43] demonstrated that B3LYP functional was more accurate than Hartree–Fock and second-order Moller–Plesset perturbation theory for Zn(II) complexes. Although a systematic comparison of methods was not the objective of the present study, additional calculations were carried out to assess the effect of the basis set and DFT functional on the relative energies. Using the 6-31G(d), single-point energies were calculated using the hybrid meta exchange–correlation functional M06 [44], i.e., M06/6-31G(d)//B3LYP/6-31G(d) (abbreviated as M06/6-31G(d)// in the present paper). The effect of the basis set on the energies was also evaluated through single-point energy calculations at the B3LYP/6-311+G(2d,p)//B3LYP/6-31G(d) (B3LYP/6-311+G(2d,p)//) and M06/6-311+G(2d,p)//B3LYP/6-31G(d) (M06/6-311+G(2d,p)//) levels. The B3LYP/6-31G(d) geometries were used in all of the calculations, and thermal corrections for energy and solvation energy were applied. The latter quantities were added to the electronic plus nuclear-repulsion energy calculated at the other levels of theory to obtain the Gibbs free energy change in gas phase and in aqueous solution, respectively.

The thermodynamic properties were calculated at 25 °C and 1 atm in the gas phase and in aqueous solution at the B3LYP/6-31G(d) level of theory. The effect of solvent on the energies was included by applying the IEFPCM continuum model [45, 46], and the macroscopic dielectric constant

was set to 78.39 (corresponding to that of water). The solute cavity was constructed according to the United Atoms scheme (UAHF) [47]. In the thermodynamic analysis, only the electrostatic contribution of the solvation energies was applied, as suggested in our previous studies [30, 32]. The calculations were performed with Gaussian 09 [48].

3 Results and discussion

TC and CMT act as MMP inhibitors via a non-antimicrobial mechanism. Specifically, TC and CMT act as a ZBG, inhibiting active MMP or MMP present in a proteinase stage. Therefore, the analysis of all possible zinc-binding modes is relevant to the design of TC derivatives with potential therapeutic applications. In the subsequent sections of the present manuscript, we discuss the structures and energies of CMT–Zn(II) complexes. First, the structures and energies of $[Zn(LH_n)(H_2O)_2]^{2-x}$ (see Eq. 1) are presented for CMT-1 and CMT-3, and the improved molecular model, $[Zn(L)(His)_3]$, which includes the first Zn(II) coordination shell of the active site of MMP-9, is discussed for five structurally related CMTs (Fig. 1).

3.1 Structure and stability of $[Zn(LH_n)(H_2O)_2]^{2-x}$

To define the most stable coordination modes of CMT–Zn(II) complexes, process (1) was investigated in the gas phase and in aqueous solution. The CMTs present different metal coordination sites, and the preferred binding sites depend on the solvent and pH of the medium. Thus, the three ionized forms of CMT-1 and CMT-3 (LH_2, LH^- and L^{2-}) were considered in the complexation processes, and 18 distinct sites were proposed for each CMT. For LH_2 and LH^-, five coordination sites were analyzed, and two distinct tautomers were proposed for sites III (O3–Nam) and IV (O1–Nam) in the LH_2 form (IIIA and IVA, respectively). Thus, a total of seven structures for $[Zn(LH_2)(H_2O)_2]^{2+}$ and five structures for $[Zn(LH)(H_2O)_2]^{+}$ were calculated. For the L^{2-} ligand, six distinct structures with a stoichiometry of $[Zn(L)(H_2O)_2]$ were proposed, and the additional coordination site involving the most frequent O11–O12 moiety, labeled site VI in Fig. 1, was only available after the second ionization at O12.

In all of the complexes, CMT-1 and CMT-3 act as bidentate ligands, except at site VI (O11–O12), which was proposed for fully deprotonated CMTs. In this case, the initial structure containing coordinated Zn(II) at O11–O12 undergoes significant distortion. In the final geometry, the Zn(II) ion is coordinated to the O11–O1 site, and a weak electrostatic interaction with the O12 moiety is observed (see Fig. 2a). The Zn–O11 and Zn–O1 bond lengths were calculated at the B3LYP/6-31G(d) level, and values of 1.94–1.97 and 1.93–1.96 Å were obtained, respectively. Alternatively, the Zn–O12 bond was between 2.16 and 2.33 Å. The Wiberg bond index (Wbi) [49], which was

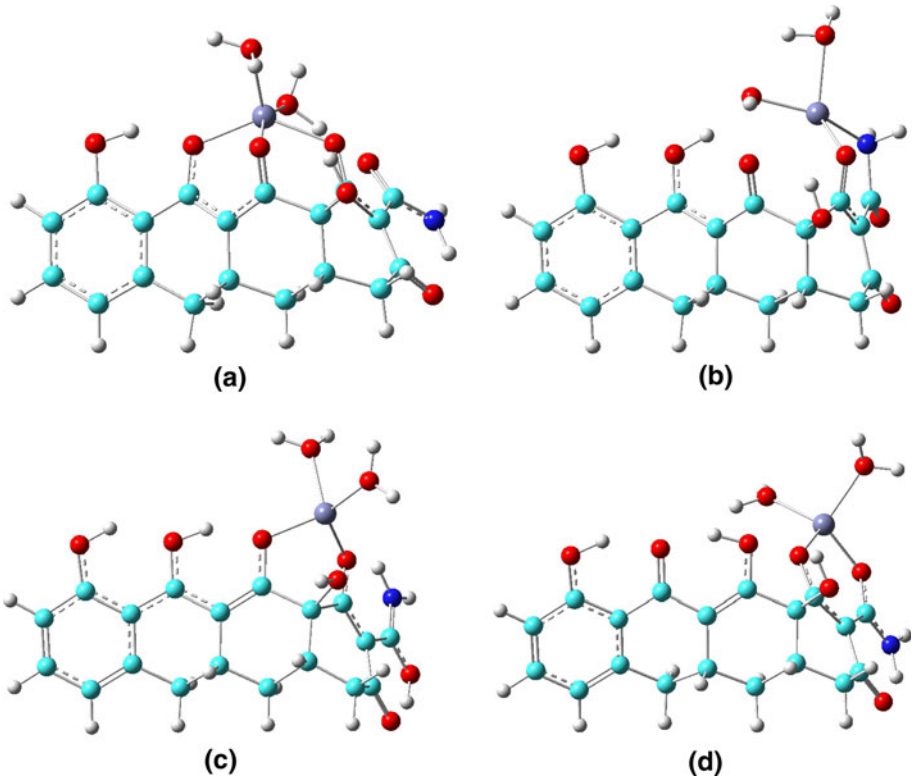

Fig. 2 B3LYP/6-31G(d) optimized structures for the most favorable complexes found for CMT-1 and CMT-3 complexes. Only the geometries for CMT-3 derivative are shown (see Supplementary materials). Sites VI (O11–O12) (**a**) and IV (O1–Oam) (**b**) for $[Zn(L)(H_2O)_2]$ complexes; site V (O1–O12) for $[Zn(LH_2)(H_2O)_2]^{2+}$ (**c**); site II (O1–Oam) for $[Zn(LH)(H_2O)_2]^{+}$ (**d**)

predicted according to Natural Bond Orbital (NBO) analysis, was equal to 0.30 for Zn–O1 and Zn–O11, and 0.14 for Zn–O12 (values for L ≡ CMT-3 in the $[Zn(L)(H_2O)_2]$ complex). Despite the relatively weak Zn–O12 interaction, the length of the bond was within the range of standard Zn–O bonds in zinc complexes with native tetracycline and zinc-metalloproteins [33, 50, 51]. Therefore, this result suggests that the CMTs act as tridentate ligands in the L^{2-} ionized state and coordinate at site VI to a pentacoordinate metal center (see Fig. 2a). The tridentate mode was previously described for a Zn(II) complex with the 5a,6-anhydrotetracycline (AHTC) analog, which was characterized by comparing experimental [51] and calculated [33] UV–Vis spectra. The predicted thermodynamic data suggested that the aforementioned structure was the preferred form in aqueous solution. In addition, a strong distortion in the skeleton of the CMT was observed upon coordination to the O11–O12–O1 site, which favored a change in the conformation of the amide group of CMT-1 and CMT-3 analogs to the *cis* form, as shown in Fig. 2a. In complex $[Zn(L)(H_2O)_2]$ coordinated at sites II (O1–Oam) and IV (O1–Nam), one proton from water was transferred to O11 during geometry optimization in the gas phase (see optimized structure IV in the Fig. 2b), leading to additional stabilization.

For complexes containing LH_2 and LH^-, CMT-1 and CMT-3 act as bidentate ligands, and the metal center presents a tetrahedral geometry (see Fig. 2c, d). The Zn–O bond lengths were 1.87–1.97 Å, and the Zn–N bond lengths were approximately 2.00–2.04 Å. The O–Zn–O angle ranged from 90.6 to 106.6°, and the O–Zn–N angle ranged from 85.4 to 96.4°. These results suggest that Zn(II) has a greater affinity for O atoms. Most of the sites described in Fig. 1 involves metal chelation at O atoms; however, in sites III (O3–Nam) and IV (O1–Nam), the N atom participates in the coordination shell. In the complex containing CMT-3 coordinated at site III (O3–Nam), the Wbi values were 0.42 and 0.29 for Zn–O3 and Zn–Nam, respectively, which supports the previous statement. Although the majority of ZBGs discussed in the literature contain oxygen atoms, some inhibitors act as nitrogen-based ZBGs [5].

As shown in Fig. 3, the relative stability of the complexes $[Zn(LH_n)(H_2O)_2]^{2-x}$ in the gas phase was compared at all of the studied levels of theory, and the most stable structure obtained at the B3LYP/6-31G(d) level was used as a reference. At low pH, LH_2 species predominated, and zinc binding occurred preferentially at site V (O12–O1). Moreover, binding was also favorable at sites I (O3–Oam) and II (O1–Oam), which are similar in energy. Site I, II and V were also quite stable when the ligand was in the LH^-, with site II (and I for CMT-3) found as global minimum. At high pH, site VI (O11–O12) was the most favorable site, followed by site II. Therefore, when the electronic plus nuclear-repulsion energy was considered, sites I, II, V and VI were more suitable for coordination to Zn(II) in the gas phase. All of the aforementioned binding sites contain only oxygen atoms; however, sites III and IV, which also contain nitrogen atom, are at least 20 kcal mol^{-1} higher in energy. As shown in Fig. 3, the order of stability did not change as the level of theory improved; therefore, only the Gibbs free energies obtained at the B3LYP/6-31G(d) level will be discussed.

The relative Gibbs free energies ($\delta\Delta G_R$) of process (1), which were calculated using B3LYP/6-31G(d) in the gas phase and in aqueous solution, are presented in Table 1. In general, the observed trends in the stability of the complexes in the gas phase and in aqueous solution were identical. For $[Zn(LH_2)(H_2O)_2]^{2+}$ complexes, the order of stability was V > II ∼ I. For $[Zn(LH)(H_2O)_2]^{+}$, sites I and II were quite favorable, and a free energy difference around 1 kcal mol^{-1} was observed in aqueous solution. For $[Zn(L)(H_2O)_2]$ complexes, site VI (O12–O11) was the most stable, and the following order was observed, regardless of the structure of the CMT: VI > I ∼ II. The stability of mode VI for complexes containing the L^{2-} ionized form was attributed to tridentate coordination mode involving O12–O11–O1 atoms (Fig. 2a). Additionally, complexes containing Zn(II) coordinated to N atoms such as III and IV were unfavorable (see values in Table 1). Nevertheless, the order of stability shown in Table 1 was identical to that shown in Fig. 3, and the contribution of thermal energy and solvation remained nearly constant. Therefore, from the results of the previous analysis, we concluded that the Zn(II) coordination site was slightly pH-dependent. Specifically, the O1–O12–O11 moiety (ring BC) was preferred at low and high pH (LH_2 and L^{2-} forms), and the O3–Oam–O1 (ring A) was favorable in neutral medium (LH^- form). Similar results were obtained in a previous study conducted on AHTC–Pt(II) complexes [31], which suggested that a rapid equilibrium was present between sites I (O3–Oam) and II (O1–Oam). In all cases, coordination sites containing only O atoms were preferred over sites containing N atom.

The previous study allowed us to identify Zn(II) preferential binding sites (II, V and VI) for CMT molecules based on the stability of complexes with CMT-1 and CMT-3 ligands. The next step was to improve the molecular model and include features from the active site of MMP-9. The function of the inhibitor is to block the active site of the enzyme; thus, the mechanism of CMT complexation with zinc must be understood.

3.2 Complexes of CMTs with catalytic zinc in the MMP-9 model

Interactions between CMTs and active zinc in MMP-9 were investigated by considering only the first metal

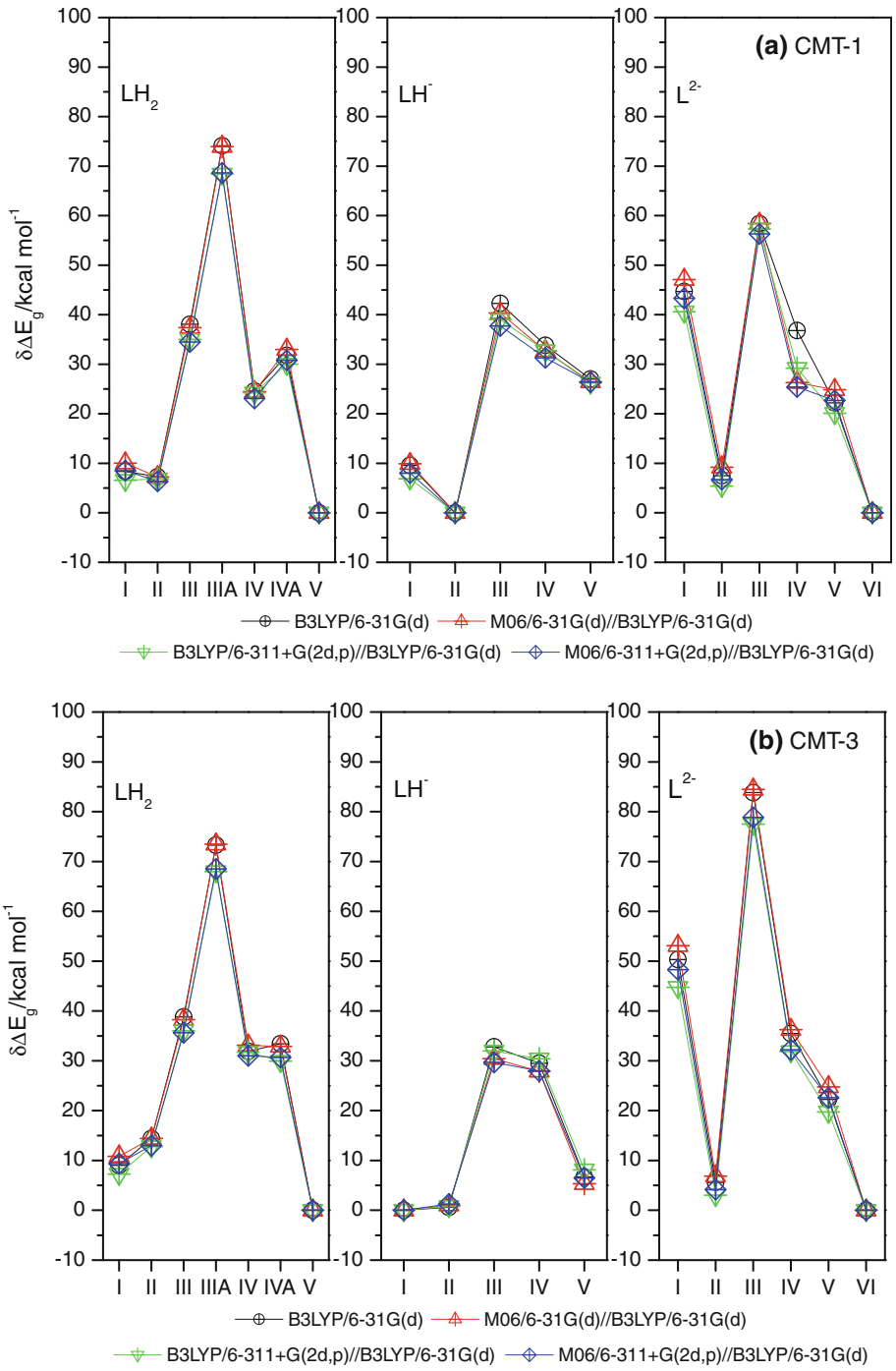

Fig. 3 Relative complexation energy calculated in gas phase for the complexes $[Zn(LH_n)(H_2O)_2]^{2-x}$ with $n = 0, 1, 2$ and $x = -2, -1, 0$

coordination shell and accounting for His401, His405 and His411. The model was obtained from the X-ray crystallographic structure of the proform of human matrix metalloproteinase MMP-9, which was solved to a resolution of 2.5 Å by Romanic and collaborators [36]. The domains were deleted, including the prodomain inserted into the active site, where the side chain of Cys99 binds to zinc in the catalytic domain. This bond is disrupted when enzyme activation occurs, allowing active zinc to interact with the substrate or inhibitors. Several studies addressing the efficacy of the application of such a simple model of the enzyme's active site have been conducted [17, 50]. The electronic structure of the metal atom and its environment play an important role in the catalytic process. Therefore, the representation of the metal and the first coordination sphere is a good approximation for studying reactions that occur at the enzyme's active site. These small models have been treated with quantum mechanics and were used to

Table 1 Relative reaction Gibbs free energy ($\delta\Delta G_R$ values in kcal mol^{-1}) in the gas phase and in aqueous solution (in brackets) calculated at B3LYP/6-31G(d) level for the distinct coordination sites of CMT-1 and CMT-3

	CMT-1			CMT-3		
	LH_2	LH^-	L^{2-}	LH_2	LH^-	L^{2-}
I (O3–Oam)	6.77 [8.63]	6.90 [1.02]	41.7 [3.00]	6.84 [8.63]	**0.00 [0.00]**	45.9 [3.52]
II (O1–Oam)	8.69 [5.15]	**0.00 [0.00]**	8.72 [10.7]	14.4 [12.0]	0.41 [1.74]	5.54 [4.79]
III (O3–Nam)	37.4 [19.1]	39.7 [22.6]	55.8 [26.8]	37.9 [19.1]	32.8 [21.7]	79.7 [26.5]
IIIA (O3–Nam)	70.6 [32.8]	–	–	70.0 [33.5]	–	–
IV (O1–Nam)	26.3 [17.2]	33.1 [20.9]	37.4 [31.1]	31.8 [22.6]	29.6 [23.2]	35.8 [29.3]
IVA (O1–Nam)	32.0 [26.9]	–	–	33.6 [28.6]	–	–
V (O1–O12)	**0.00 [0.00]**	25.5 [19.2]	21.7 [8.18]	**0.00 [0.00]**	8.03 [15.3]	21.2 [7.86]
VI (O11–O12)	–	–	**0.00 [0.00]**	–	–	**0.00 [0.00]**

The most stable structure was used as reference for each ionized state

The lowest energy values, set to zero, are emphasized in bold

study the structure and mechanism of several enzymes [6, 17, 52]. Thus, to define the preference of the CMT site for complexation with zinc, the simplified model of the enzyme is sufficient.

CMT-1, CMT-3, CMT-4, CMT-7 and CMT-8 in the L^{2-} ionized form were evaluated, and all of the coordination sites were considered to be accessible. Based on the results obtained for the $[Zn(LH_n)(H_2O)_2]^{2-x}$ complexes, only the most stable coordination sites were considered, including sites II (O1–Oam), V (O12–O1) and VI (O11–O12). The geometries of the free ligands (CMTs) and the Zn(II) complexes (a total of 21 distinct structures) were fully optimized using B3LYP/6-31G(d). In addition, the energies of the complexes were calculated at the B3LYP/6-311+G(2d,p)// level and using modern meta exchange–correlation functional M06 with 6-31G(d) and 6-311+G (2d,p) basis sets. The thermodynamic parameters of reaction (2) are discussed, as well as the energies and structures of the distinct complexes.

$$[Zn(His)_3]^{2+} + L^{2-} \rightarrow [Zn(L)(His)_3] \quad (2)$$

The metal–ligand bond lengths and angles were compared to actual models obtained from the X-ray structure [36].

Before discussing the energy of the complexation modes, some structural characteristics of the complexes must be considered. In all of the structures, the coordination moieties involve O atoms, and the CMTs act as bidentate ligands. Additionally, the conformational flexibility of tetracyclines allows them to adopt different forms, according to the solvent type and pH of the medium [52]. Particularly, the extended (EXT) to folded (FLD) interconversion process (Fig. 4 inside) was considered, which involves a pseudo-rotation of the C4a–C12a bond and can be tracked through the value of the dihedral angle

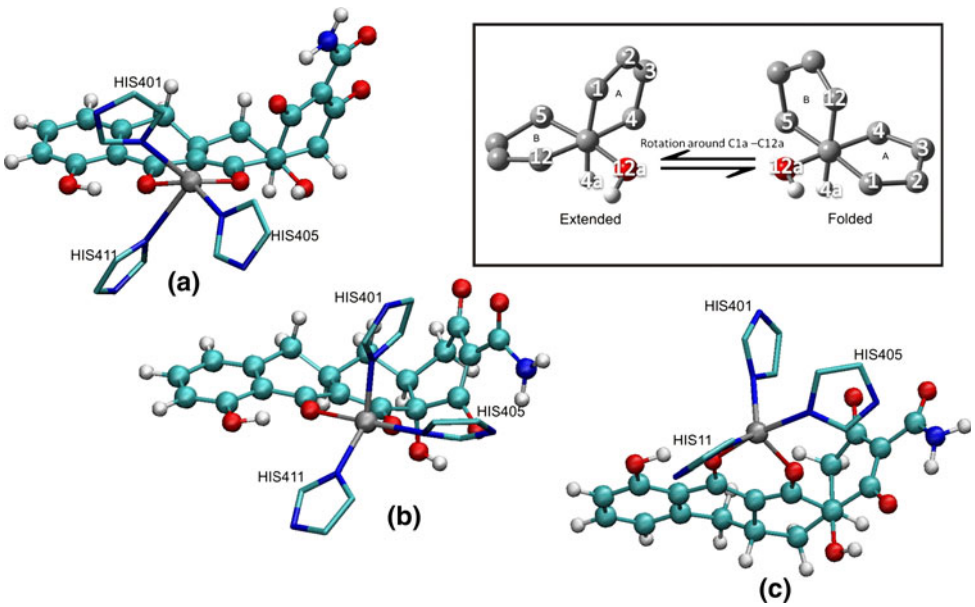

Fig. 4 Representation of the extended (**a**) → folded (**c**) conformational interconversion predicted for the CMT-3-Zn(II) complex. The intermediate structure shown in **b** was taken after 72 optimization steps

O12a–C12a–C4a–H4a (ω_1) (see Fig. 1 for the numbering scheme). In the EXT form, ω_1 is between 50 and 60°, and the value of the FLD conformer is around −60° [53]. Theoretical studies indicate that these geometries differ in energy by only a few kcal mol^{-1} [25, 27, 54]; therefore, it is practically impossible to identify conditions under which one species is present exclusively. The TCs can also change their conformation upon metal complexation. Distinct complexation sites are available for different spatial forms of the TC ligand [27].

In [Zn(L)$(His)_3$] complexes, a conformational change from EXT to FLD was predicted for L = CMT-3. Figure 4 shows snapshots obtained from the optimization of the geometry of [Zn(CMT-3)$(His)_3$] in mode VI, and the EXT → FLD process was clearly followed. In the initial structure (Fig. 4a), $\omega_1 = 47.2°$ and the structure was assigned as EXT, according to ref. [53]. In the intermediate geometry obtained after 72 optimization steps (Fig. 4b), we found $\omega_1 = 5.5°$. Alternatively, for the final optimized structure, (Fig. 4c) $\omega_1 = -60.8°$, and the conformation was assigned as FLD. Interconversion was favored by strong hydrogen bond between the O3 atom and the amino group of His411 (O3···HNH(His411) = 1.95 Å). A secondary interaction responsible for the stabilization of FLD involves the Nam amide moiety and the HN of His405 (H_2N···HN(His405) = 2.0 Å). However, these interactions are more difficult to attain in the protein active site, where the flexibility of amino acids is lower.

Table 2 presents structural parameters of the compounds, which were calculated at the B3LYP/6-31G(d) level. The Zn-ligand bond lengths were approximately 2.1 Å, regardless of the ligand type, suggesting that the coordination number of Zn(II) was five. An interesting structural aspect is the degree of trigonality (τ) of the zinc metal center in the complexes. This quantity is computed as $\tau = (\beta-\alpha)/60°$, where β is the angle formed by the axial ligands and α is the largest angle along the basal (equatorial) plane. For $\tau = 1$, the structure can be viewed as a perfect D_{3h} trigonal bipyramid. Alternatively, for $\tau = 0$, the structure was assigned as C_{4v} square pyramidal [55].

The analysis of the parameter τ (see Table 2) reveals interesting trends in the coordination of the zinc ion in the A ring of the CMTs to site II (O1–Oam). The degree of trigonality is close to zero for most of the complexes, especially CMT-1 and CMT-3 ($\tau = 0.1$) (Fig. 5a), which suggests that the geometry around the metal center was almost perfectly square pyramidal. Conversely, CMT complexes involving site V (O12–O1) and VI (O11–O12) show a degree of trigonality close to 1.0. In particular, in the CMT-3 complex, the degree of trigonality reached 0.8 (see Fig. 5b). These complexes involve coordination at the A, B or C rings of the CMT ligands. In these cases, the geometry around the metal center was nearly perfectly trigonal bipyramidal. These results suggested that the geometry of zinc depends on the ligand-binding site, not the CMT. As previously discussed [56], the zinc ion may

Table 2 Structural parameters calculated at B3LYP/6-31G(d) for the [Zn(L)$(His)_3$] complexes with L corresponding to distinct CMTs

	Molecules	Zn–O[a]	Zn–N(His401)	Zn–N(His405)	Zn–N(His411)	∠N(His401)–Zn–N(His405)	∠N(His411)–Zn–O[a]	τ
X-ray	MMP-9[b]	–	2.05	2.21	2.26	107.3	–	–
II (O1–Oam)	CMT-1	2.07	2.04	2.07	2.10	116.6	151.8	0.13
	CMT-3	2.00	2.04	2.06	2.27	107.5	157.7	0.11
	CMT-4	2.08	2.05	2.06	2.15	120.8	159.6	0.37
	CMT-7	2.02	2.05	2.10	2.12	136.3	174.6	0.64
	CMT-8	2.03	2.05	2.06	2.19	118.1	164.8	0.52
V (O12–O1)	CMT-1	2.03	2.05	2.11	2.16	134.9	173.8	0.65
	CMT-3	2.03	2.08	2.09	2.21	105.9	171.4	0.68
	CMT-4	2.07	2.05	2.10	2.10	127.6	170.6	0.72
	CMT-7	2.01	2.06	2.12	2.15	133.8	172.3	0.64
	CMT-8	2.02	2.07	2.08	2.17	128.2	180.0	0.86
VI (O11–O12)	CMT-1	2.04	2.03	2.06	2.16	115.7	171.0	0.89
	CMT-3	2.05	2.06	2.07	2.14	124.7	170.2	0.76
	CMT-4	2.04	2.06	2.06	2.14	112.2	168.8	0.74
	CMT-7	2.03	2.05	2.07	2.16	114.2	170.5	0.66
	CMT-8	2.00	2.04	2.08	2.19	115.3	166.2	0.72

Only the sites II (O1–Oam), V (O1–O12) and VI (O11–O12) are considered. The bond lengths are in Å and the bond angles in degrees

[a] Average bond length is reported

[b] Values from the X-ray crystallographic structure (PDB code 1L6J) [36]

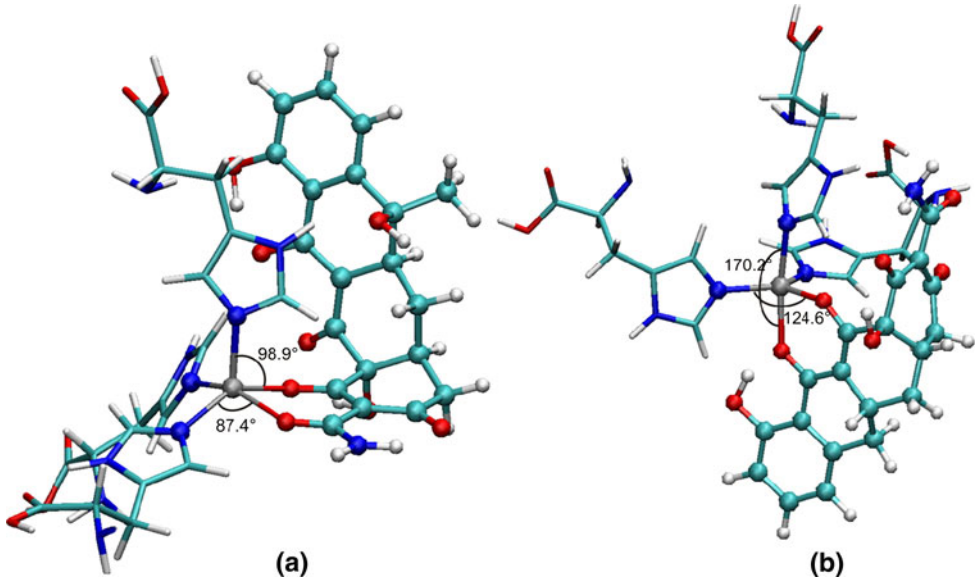

Fig. 5 B3LYP/6-31G(d) optimized structure of the complexes [Zn(L)(His)$_3$] with L being CMT-1 (**a**) and CMT-3 (**b**). The values inside are the bond angles used to calculate the degree of trigonality

assume different geometries, depending on the coordination site. The X-ray crystallography [7] of hydroxamate MMP inhibitors has been studied, and the results revealed that the catalytic zinc ion in MMP-9 coordinates to His401, His405, His411 and both hydroxamate oxygen atoms. The geometry around the metal was assigned as distorted pentacoordinate and was close to perfectly square pyramidal ($\tau = 0.1$). The X-ray crystallography [57] structure of MMP-9 coordinated to a carboxylate inhibitor similar to CMT was also evaluated, and the results showed that the metal had a coordination number of five and a nearly perfect square pyramidal geometry ($\tau = 0.1$). Thus, based only on the overall geometry of the first coordination sphere around the metal center, we hypothesized that coordination site II of the CMTs was more suitable for binding to the MMP-9 catalytic site than the other sites. For instance, when coordinated at site II, CMT-1 and CMT-3 interact with the imidazole ring of histidine (His401) residues, which decreases the angle of His401–Zn–O and His411–Zn–O (see Table 2) and reduces the degree of trigonality.

Table 3 shows the Gibbs free energy of the process illustrated in Eq. 2 in the gas phase ($\Delta G_{R,g}$) and in aqueous solution ($\Delta G_{R,aq}$) for all of the [Zn(L)(His)$_3$] complexes. In general, all of the processes were favorable, except when the B3LYP/6-311+G(2d,p)// level was applied, and several positive values for $\Delta G_{R,aq}$ were obtained. The order of stability depends on the coordination site and the ligand structure. According to all of the methods, the most spontaneous zinc-binding moiety in the gas phase was site II (O1–Oam) for CMT-1, -4, -7 and -8, and site VI (O11–O12) for CMT-3. This trend was also observed in solution, except when the triple-zeta quality basis set was applied to CMT-8. In this case, site VI was the main coordination site in solution. In addition, sites II (CMT-1, -4 and -7) and VI (CMT-3 and -8) are preferable for Zn(II) ion binding in aqueous solution. The Gibbs free energy of the reaction in solution accounts for three contributions; namely, $\Delta G_{R,aq} = \Delta E_{R,g} + \delta G_T + \delta G_{solv}$, where the first term on the right is the reaction energy in the gas phase, including the electronic plus nuclear-repulsion contributions, and the last two terms are thermal corrections applied to the Gibbs free energy (including zero point energy, enthalpic and entropic contributions) and solvation contributions of the reaction, respectively. In the present study, only $\Delta E_{R,g}$ was calculated at every level of theory, and δG_T and δG_{solv} were calculated according to B3LYP/6-31G(d). As shown in Table 3, the solvent plays a significant role in the spontaneity of the process because the reactants are charged and the products are neutral species (Eq. 2). Therefore, in the PCM approach, the solvation energies of the former are more pronounced, which raises the final free energy of the reaction. Despite the drawbacks in the continuum solvation method regarding the description of ionic species, the results obtained in solution appear to be reasonable compared to similar processes with tetracycline-like molecules [51]. Before describing the structure–reactivity relationships, the effect of the level of theory on the reaction energy must be highlighted. The reaction energies calculated with M06 functional were 4–7% lower (more negative values) than the corresponding B3LYP data. Alternatively, as the basis set increased, the reaction energies increased by 8–9%; therefore, the values calculated at M06/6-311+G(2d,p)// provided optimal results, accounting for both types of effects. Thus, only these values will be discussed hereafter (last two columns in Table 3).

As previously described, the reaction between Zn(II) and CMT-1 occurs preferentially at site II. Alternatively, for

Table 3 Reaction Gibbs free energy (in kcal mol^{-1}) for the complexes [Zn(L)(His)$_3$] with L = CMT-1, -3, -4, -7 and -8

	$\Delta G_{R,g}$ [$\Delta G_{R,aq}$][a,b]				log β[c,d]
	B3LYP/6-31G(d)	M06/6-31G(d)//	B3LYP/6-311+G(2d,p)//	M06/6-311+G(2d,p)//	M06/6-311+G(2d,p)//
CMT-1					
II (O1–Oam)	**−286.5 [−28.3]**	**−300.8 [−42.7]**	**−263.7 [−5.55]**	**−283.1 [−24.9]**	18.3
V (O1–O12)	−257.4 [−14.1]	−272.5 [−29.3]	−238.2 [5.06]	−257.1 [−13.9]	10.2
VI (O11–O12)	−261.5 [−17.8]	−271.9 [−28.2]	−241.9 [1.77]	−255.9 [−12.3]	9.0
CMT-3					
II (O1–Oam)	−284.2 [−20.7]	−299.4 [−37.0]	−262.4 [0.00]	−282.8 [−20.5]	15.0
V (O1–O12)	−257.4 [−8.36]	−269.6 [−21.7]	−237.8 [10.0]	−253.8 [−5.92]	4.3
VI (O11–O12)	**−293.6 [−24.5]**	**−308.3 [−40.4]**	**−269.0 [−1.00]**	**−289.7 [−21.7]**	15.9
CMT-4					
II (O1–Oam)	**−293.7 [−27.9]**	**−312.4 [−48.8]**	**−269.5 [−5.91]**	**−294.9 [−31.3]**	23.0
V (O1–O12)	−270.7 [−17.4]	−287.7 [−36.7]	−249.3 [1.71]	−271.8 [−20.8]	15.3
VI (O11–O12)	−272.7 [−16.2]	−288.2 [−34.0]	−251.7 [2.55]	−272.9 [−18.6]	13.6
CMT-7					
II (O1–Oam)	**−274.1** [−13.9]	**−293.7 [−35.0]**	**−250.7** [8.08]	**−276.8 [−18.1]**	13.3
V (O1–O12)	−262.6 **[−18.0]**	−276.2 [−33.1]	−243.2 **[−0.03]**	−260.5 [−17.3]	12.7
VI (O11–O12)	−257.5 [−16.1]	−268.9 [−29.0]	−238.8 [1.07]	−253.7 [−13.8]	10.1
CMT-8					
II (O1–Oam)	**−285.9 [−23.3]**	**−304.1 [−43.5]**	**−261.1** [−0.50]	**−286.3** [−25.7]	18.8
V (O1–O12)	−266.3 [−22.6]	−279.8 [−38.1]	−245.5 [−3.83]	−252.0 [−10.3]	7.6
VI (O11–O12)	−258.2 [−22.5]	−267.6 [−33.9]	−239.5 **[−5.82]**	−262.7 **[−29.0]**	21.3

The log β calculated in aqueous solution are also included, where β is the formation constant calculated according to the process represented in Eq. 2

The reaction energies for the most stable sites are emphasized in bold

[a] Reaction Gibbs free energies are calculated as $\Delta G_{R,aq} = \Delta E_{R,g} + \delta G_T + \delta G_{solv}$, where δG_T and δG_{solv}, are the thermal correction and solvation energy for the reaction calculated at B3LYP/6-31G(d) level. The $\Delta G_{R,g}$ is the sum of the two first terms on the right

[b] The double slashes used in the notation for the level of theory indicate single-point energy calculation using the B3LYP/6-31G(d) optimized geometry

[c] Calculated using the M06/6-311+G(2d,p)// values. The log $\beta = -\Delta G_{R,aq}/1.364$ ($T = 298$ K)

[d] The experimental value is log $\beta = 15.59 \pm 0.01$ for the AHTC–Zn(II) complex [51]

CMT-3, structure VI was slightly favored over site II (1.2 kcal mol^{-1}). The values obtained in solution for CMT-1 and CMT-3 (Tables 1, 3) were compared. For CMT-3, similar trends were observed, namely, site VI was more stable, regardless of the model. However, for CMT-1, site II was 12.6 kcal mol^{-1} lower in energy than site VI when the biological model was considered. The order of stability of CMT-4 complexes was identical to those predicted for CMT-1 (II > V ~ VI, see Table 3). The structures of these molecules are similar and differ only at the C7. For CMT-7, structure II was also more stable; however, site V was significantly stabilized and was only 0.8 kcal mol^{-1} less stable than site II in aqueous solution. Unlike CMT-1, CMT-7 does not contain an OH at C12a, which may interfere with coordination at site V (see Fig. 1).

The structure–reactivity relationship for CMT-8 complexes was similar to that of CMT-3, and the following order in the stability was observed: VI > II ≫ V. A common feature among these structures is a lack of hydroxyl groups at C6. CMT-8 bears an OH group at C5 and resembles the parent DOX tetracycline (see Fig. 1). The interaction between AHTC analogs and the Zn(II) ion in aqueous solution was studied by Beraldo et al. [51] via absorption and circular dichroism (CD) spectroscopy. The results of the aforementioned study suggested that site VI (O11–O12) was the primary coordination site, and the formation constant of the AHTC-Zn(II) complex was (in logarithmic scale) equal to log $\beta = 15.59 \pm 0.01$. Table 3 shows the formation constants calculated at the M06/6-311+G(2d,p)// level for the interaction between CMTs and active zinc in aqueous solution. Although differences between the experimental and theoretical results were observed, the formation constants of the most stable complexes were comparable. Furthermore, the experimental results suggested that site VI (O11–O12) was involved in the coordination of TC analogs with active

zinc, which is quite favorable for CMT-3 (log $\beta = 15.9$) and CMT-8 (log $\beta = 21.3$). The main difference between the CMT ligands is the absence of an OH group at C6 in CMT-3 and CMT-8, which stabilizes site VI. Similarly, the tetracycline-based antibiotic doxycycline (DOX) [8, 10, 11], which is an effective MMP inhibitor, does not contain an OH group at the C6 position of the C ring, which suggests that the presence of OH hinders coordination at site O11–O12.

At present, the molecular mechanism of MMP inhibition by CMTs has not been completely described. However, structure–activity relationships in the CMTs have been observed. For instance, structural differences among CMTs affect the ability of the compound to interact with protease sites [8, 15]. In the present study, we demonstrated that the structure of the CMTs interferes with coordination to Zn(II) at the active site. Based on the relative energies shown in Table 3, CMT-3 and CMT-8 analogs, which are derivatives that bind preferentially to Zn(II) at site VI (O11–O12), displayed singular behavior. For the other CMTs, chelation was more favorable at site II or V (see Table 3). Therefore, considering the simplest model for active zinc reacting with a set of chemically modified tetracyclines, the structural and energetic properties determined in the present study suggest that CMT-3 and CMT-8 present different Zn(II)-coordination properties, which may be related to the distinct activity of these analogs as MMP inhibitors.

4 Concluding remarks

In the present study, DFT calculations were applied to describe coordination processes involving Zn(II) and chemically modified tetracyclines (CMTs). Two molecular models were considered in the first metal coordination shell, including water (chemical model) and amino acids (biological model), which mimic the MMP-9 catalytic site. The results of the chemical model indicated that the binding mode depends on the protonation state of the ligand. The O1–O12–O11 moiety (ring BC) was preferred at low and high pH (LH_2 and L^{2-} forms), and O3–Oam–O1 (ring A) was favorable in neutral medium (LH^- form). In the biological model, the complexes included $[Zn(L)(His)_3]$ in the fully deprotonated form, where L = CMT-1, CMT-3, CMT-4, CMT-7 and CMT-8. Among these CMTs, the most important was CMT-3, which demonstrated significant activity as an MMP inhibitor, and CMT-8, which is a direct derivative of DOX, the only FDA-approved MMPI. For these analogs, coordination site VI (O11–O12) was the most favorable in solution (log $\beta > 15$). This result suggests that CMT-3 and CMT-8 should coordinates to MMP-9 stronger than the other CMTs. In addition, a pentacoordinated Zn(II) complex was also predicted, and a distorted bipyramid trigonal geometry with $\tau \sim 0.8$ was assumed. For the other derivatives, log β was approximately 9–13 when site VI was included. Thus, the OH group at C6 reduces the stability of complex VI, favoring sites II and V. For CMT-1 and CMT-4, which differ only at C7, site II was favorable, and log β was equal to 18.3 and 23.0, respectively. These features may play a role in the abilities of the ligands to bind to the enzyme's active site. The systematic evaluation of the relationship between the molecular properties of CMTs and their interaction with the catalytic Zn(II) ion in matrix metalloproteinase could aid in the understanding of their mechanism of action as MMP inhibitors and the design of new analogs with enhanced biological potency.

Acknowledgments The authors thank the Conselho Nacional de Desenvolvimento Científico (CNPq—479682/2008-9) by the provision of the research concessions and for the financial support; and to Fundação de Amparo à Pesquisa do Estado de Minas Gerais (FAPEMIG—CEX—APQ-00498-08) by the fomentation. B. L. Marcial also thanks to the CAPES for graduate fellowship.

References

1. Nuti E, Tuccinardi T, Rossello A (2007) Curr Pharm Des 13:2087–2100
2. Murphy G, Nagase H (2008) Mol Aspects Med 29:290–308
3. Roy R, Yang J, Moses MA (2009) J Clin Oncol 27:5287–5297
4. Tu GG, Xu WF, Huang HM, Li SH (2008) Curr Med Chem 15:1388–1395
5. Jacobsen JA, Jourden JLM, Miller MT, Cohen SM (2010) Biochim Biophys Acta 1803:72–94
6. Gupta SP (2007) Chem Rev 107:3042–3087
7. Rowsell S, Hawtin P, Minshull CA, Jepson H, Brockbank SMV, Barratt DG, Slater AM, McPheat WL, Waterson D, Henney AM, Pauptit RA (2002) J Mol Biol 319:173–181
8. Acharya MR, Venitz E, Figg WD, Sparreboom A (2004) Drug Resist. Updates 7:195–208
9. Syed S, Takimoto C, Hidalgo M, Rizzo J, Kuhn JG, Hammond LA, Schwartz G, Tolcher A, Patnaik A, Eckhardt SG, Rowinsky EK (2004) Clin Cancer Res 10:6512–6521
10. Lee H, Park JW, Kim SP, Lo EH, Lee SR (2009) Neurobiol Dis 34:189–198
11. Shen LC, Chen YK, Lin LM, Shaw SY (2010) Oral Oncol 46:178–184
12. Greenwald RA, Golub LM (2001) Curr Med Chem 8:237–242
13. Sandler C, Nurmi K, Lindstedt KA, Sorsa T, Golub LM, Kovanen PT, Eklund KK (2005) Int Immunopharmacol 5:1611–1621
14. Seftor REB, Seftor EA, De Larco JE, Kleiner DE, Leferson J, Stetler-Stevenson WG, McNamara TF, Golub LM, Hendrix MJC (1998) Clin Exp Metastasis 16:217–225
15. Liu Y, Ramamurthy NS, Marecek J, Lee HM, Chen JL, Ryan ME, Rifkin BR, Golub LM (2001) Curr Med Chem 8:243–252
16. Islam MM, Franco CD, Courtman DW, Bendeck MP (2003) Am J Pathol 163:1557–1566
17. Diaz N, Suarez D, Sordo TL (2006) J Phys Chem B 110:24222–24230
18. Aly AAM, Strasser A, Vogler A (2002) Inorg Chem Commun 5:411–413

19. Asleson GL, Frank CW (1975) J Am Chem Soc 97:6246–6248
20. De Siqueira JM, Carvalho S, Paniago EB, Tosi L, Beraldo H (1994) J Pharm Sci 83:291–295
21. Guerra W, Silva IR, Azevedo EA, Monteiro A, Bucciarelli-Rodriguez M, Chartone-Souza E, Silveira JN, Fontes APS, Pereira-Maia EC (2006) J Braz Chem Soc 17:1627–1633
22. Lee JY, Everett GW (1981) J Am Chem Soc 103:5221–5225
23. Machado FC, Demicheli C, Garniersuillerot A, Beraldo H (1995) J Inorg Biochem 60:163–173
24. Wessels JM, Ford WE, Szymczak W, Schneider S (1998) J Phys Chem B 102:9323–9331
25. Meindl K, Clark T (2005) J Phys Chem B 109:4279–4284
26. Leypold CF, Marian DT, Roman C, Schneider S, Schubert P, Scholz O, Hillen W, Clark T, Lanig H (2004) Photochem Photobiol Sci 3:109–119
27. Othersen OG, Lanig H, Clark T (2006) J Mol Model 12:953–963
28. Aleksandrov A, Simonson T (2006) J Comput Chem 27: 1517–1533
29. Duarte HA, Carvalho S, Paniago EB, Simas AM (1999) J Pharm Sci 88:111–120
30. Marcial BL, Costa LAS, De Almeida WB, Dos Santos HF (2008) J Braz Chem Soc 19:1437–1449
31. Dos Santos HF, Marcial BL, De Miranda CF, Costa LAS, De Almeida WB (2006) J Inorg Biochem 100:1594–1605
32. Marcial BL, Costa LAS, De Almeida WB, Dos Santos HF (2009) J Mol Struct (Theochem) 916:94–104
33. Dos Santos HF, De Almeida WB, Zerner MC (1998) J Chem Soc Perkin Trans 2:2519–2525
34. Dos Santos HF, Xavier ES, Zerner MC, De Almeida WB (2000) J Mol Struct (Theochem) 527:193–202
35. De Almeida WB, Dos Santos HF, Zerner MC (1998) J Pharm Sci 87:1101–1108
36. Elkins PA, Ho YS, Smith WW, Janson CA, D'Alessio KJ, McQueney MS, Cummings MD, Romanic AM (2002) Acta Crystallogr D Biol Crystallogr 58:1182–1192
37. Pinsuwan S, Alvarez-Nunez FA, Tabibi SE, Yalkowsky SH (1999) J Pharm Sci 88:535–537
38. Becke AD (1988) Phys Rev A 38:3098–3100
39. Lee CT, Yang WT, Parr RG (1988) Phys Rev B 37:785–789
40. Curtiss LA, Raghavachari K, Redfern PC, Rassolov V, Pople JA (1998) J Chem Phys 109:7764–7776
41. Rassolov VA, Ratner MA, Pople JA, Redfern PC, Curtiss LA (2001) J Comput Chem 22:976–984
42. Sousa SF, Carvalho ES, Ferreira DM, Tavares IS, Fernandes PA, Ramos MJ, Gomes J (2009) J Comput Chem 30:2752–2763
43. Sousa SF, Fernandes PA, Ramos MJ (2007) J Phys Chem A 111:10439–10452
44. Zhao Y, Truhlar DG (2008) Theor Chem Acc 120:215–241
45. Cances E, Mennucci B, Tomasi J (1997) J Chem Phys 107:3032–3041
46. Cossi M, Scalmani G, Rega N, Barone V (2002) J Chem Phys 117:43–54
47. Barone V, Cossi M, Tomasi J (1997) J Chem Phys 107:3210–3221
48. Frisch MJ, Trucks GW, Schlegel HB, Scuseria GE, Robb MA, Cheeseman JR, Scalmani G, Barone V, Mennucci B, Petersson GA, Nakatsuji H, Caricato M, Li X, Hratchian HP, Izmaylov AF, Bloino J, Zheng G, Sonnenberg JL, Hada M, Ehara M, Toyota K, Fukuda R, Hasegawa J, Ishida M, Nakajima T, Honda Y, Kitao O, Nakai H, Vreven T, Montgomery JA Jr, Peralta JE, Ogliaro F, Bearpark M, Heyd JJ, Brothers E, Kudin KN, Staroverov VN, Kobayashi R, Normand J, Raghavachari K, Rendell A, Burant JC, Iyengar SS, Tomasi J, Cossi M, Rega N, Millam NJ, Klene M, Knox JE, Cross JB, Bakken V, Adamo C, Jaramillo J, Gomperts R, Stratmann RE, Yazyev O, Austin AJ, Cammi R, Pomelli C, Ochterski JW, Martin RL, Morokuma K, Zakrzewski VG, Voth GA, Salvador P, Dannenberg JJ, Dapprich S, Daniels AD, Farkas Ö, Foresman JB, Ortiz JV, Cioslowski J, Fox DJ (2009) Gaussian 09, revision A.1. Gaussian, Inc., Wallingford
49. Wiberg KB (1968) Tetrahedron 24:1083–1096
50. Tamames B, Sousa SF, Tamames J, Fernandes PA, Ramos MJ (2007) Proteins: Struct Funct Bioinform 69:466–475
51. Matos S, Beraldo H (1995) J Braz Chem Soc 6:405–411
52. Linder DP, Rodgers KR (2004) J Phys Chem B 108:13839–13849
53. Dos Santos HF, Nascimento CS, Belletato P, De Almeida WB (2003) J Mol Struct (Theochem) 626:305–319
54. Dos Santos HF, De Almeida WB, Zerner MC (1998) J Pharm Sci 87:190–195
55. Addison AW, Rao TN, Reedijk J, Vanrijn J, Verschoor GC (1984) J Chem Soc Dalton Trans 4:1349–1356
56. Sousa SF, Lopes AB, Fernandes PA, Ramos MJ (2009) Dalton Trans 48:7946–7956
57. Tochowicz A, Maskos K, Huber R, Oltenfreiter R, Dive V, Yiotakis A, Zanda M, Bode W, Goettig P (2007) J Mol Biol 371:989–1006